International Journal of Solids and Structures 46 (2009) 4073–4078

Contents lists available at ScienceDirect

International Journal of Solids and Structures

journal homepage: www.elsevier.com/locate/ijsolstr

The thermoelastic Hertzian contact problem

Yong Hoon Jang [a,*], Hanbum Cho [b], J.R. Barber [c]

[a] School of Mechanical Engineering, Yonsei University, 134 Shinchon-dong, Seodaemun-gu, Seoul 120-749, Republic of Korea
[b] Orrick, Herrington & Sutcliffe LLP, 1000 Marsh Road, Menlo Park, CA 94025, USA
[c] Department of Mechanical Engineering and Applied Mechanics, University of Michigan, Ann Arbor, MI 48109-2125, USA

ARTICLE INFO

Article history:
Received 21 April 2009
Received in revised form 24 June 2009
Available online 11 August 2009

Keywords:
Hertzian contact
Thermoelastic contact
Thermal contact resistance
Thermoelasticity

ABSTRACT

A numerical solution is obtained for the steady-state thermoelastic contact problem in which heat is conducted between two elastic bodies of dissimilar materials at different temperatures with arbitrary quadratic profiles. Thermoelastic deformation causes the initially elliptical contact area to be reduced in size and to become more nearly circular as the temperature difference is increased. There is also a small but identifiable deviation from exact ellipticity at intermediate temperature differences. An approximate analytical solution is obtained, based on approximating the contact area by an ellipse.

1. Introduction

When two conforming bodies are placed in contact, the contact pressure distribution is sensitive to comparatively small changes in surface profile. Thermoelastic deformations, though generally small, can therefore have a significant effect on systems involving contact. For example, Clausing (1966) showed experimentally that the thermal contact resistance between two contacting bodies varied with the transmitted heat flux as a result of thermoelastically driven changes in the extent of the contact area.

If the contacting bodies are small, their surfaces can be approximated by quadratic functions in the vicinity of the contact area and in the absence of thermoelastic deformation, the solution of the elastic contact problem is given by the classical Hertz theory (Johnson, 1985). In particular, the contact area is an ellipse whose ellipticity and orientation are unique functions of the coefficients defining the quadratic surfaces and whose linear dimensions vary with $P^{1/3}$, where P is the contact force.

If the extremities of the two bodies are now raised to different temperatures T_1, T_2, heat will flow through the contact area and the resulting thermoelastic deformation will influence the contact area and the contact pressure distribution. This problem was solved by Barber (1973) for the special case where the bodies are axisymmetric. In this case, the contact area is always circular and its radius a for a given contact force decreases with increasing temperature difference, being given by

$$\hat{a}^3 + \frac{3\Theta\hat{a}^2}{2\pi} = 1, \tag{1}$$

where

$$\hat{a} = \frac{a}{a_H}, \quad \Theta = \frac{(\delta_2 - \delta_1)(T_1 - T_2)KR}{a_H}, \quad \frac{1}{K} = \frac{1}{K_1} + \frac{1}{K_2}, \quad \frac{1}{R} = \frac{1}{R_1} + \frac{1}{R_2}, \tag{2}$$

a_H is the radius of the isothermal (Hertzian) elastic contact area for the same contact force P, R_1, R_2 are the radii of the two contacting bodies and the distortivity δ is defined as

$$\delta = \frac{\alpha(1+\nu)}{K}, \tag{3}$$

where α, ν, K are the coefficient of thermal expansion, Poisson's ratio and thermal conductivity. This solution is strictly only applicable when the heat flows into the body with the higher distortivity and hence the dimensionless parameter $\Theta > 0$, since for the opposite direction of heat flow, a small annulus of imperfect thermal contact is developed at the edge of the contact area (Barber, 1978; Kulchytsky-Zhyhailo et al., 2001).

In this paper, we use a numerical method to determine the effect of thermoelastic deformation for the more general Hertzian case where the bodies have general quadratic shapes and the isothermal contact area is elliptical. We shall show that the contact area becomes smaller and also more nearly circular as the temperature difference is increased. We shall also develop an approximate analytical solution to the problem, using an approach proposed by Yevtushenko and Kulchytsky-Zhyhailo (1996).

* Corresponding author. Tel.: +82 2 2123 5812; fax: +82 2 312 2159.
E-mail address: jyh@yonsei.ac.kr (Y.H. Jang).

0020-7683/$ - see front matter © 2009 Elsevier Ltd. All rights reserved.
doi:10.1016/j.ijsolstr.2009.08.004

2. Statement of the problem

We consider the problem in which two thermally conducting elastic bodies are pressed together by a force P, whilst their extremities are maintained at temperatures T_1 and T_2, respectively. Frictionless contact conditions are assumed and heat flow between the elastic bodies is only permitted to take place by conduction through the contact area A. As in the axisymmetric case, we restrict attention to the case where the heat flows into the more distortive material and hence $(T_1 - T_2)(\delta_1 - \delta_2) < 0$.

2.1. The heat conduction problem

The temperature at the point defined by coordinates (x, y) on the surface of body i can be written as

$$T_i(x,y) = \frac{1}{2\pi K_i}\int\int \frac{q(\xi,\eta)d\xi d\eta}{r} + T_i \tag{4}$$

where q is the heat flux directed into the body and

$$r = \sqrt{(x-\xi)^2 + (y-\eta)^2}. \tag{5}$$

In the absence of surface tractions, this heat flux would also cause thermoelastic displacement w_i in the inward normal direction given by (Barber, 1971)

$$w_i(x,y) = \frac{\delta_i}{2\pi}\int\int q(\xi,\eta)\ln(r)d\xi d\eta, \tag{6}$$

where we have omitted a rigid-body displacement.

Continuity of heat flux and temperature at the contact area then leads to the integral equation

$$\Delta T \equiv T_1 - T_2 = \frac{1}{2\pi K}\int\int_A \frac{q(\xi,\eta)d\xi d\eta}{r}, \tag{7}$$

where K is defined in Eq. (2). This equation serves to determine the heat flux q, which is here taken as positive in the direction from body 1 to body 2. Once q is determined, the differential thermoelastic expansion can then be determined from Eq. (6) as

$$w_1(x,y) + w_2(x,y) = \frac{(\delta_2 - \delta_1)}{2\pi}\int\int q(\xi,\eta)\ln(r)d\xi d\eta. \tag{8}$$

2.2. The contact problem

We suppose that the two contacting bodies have profiles defined by the functions $g_1(x,y), g_2(x,y)$, as shown in Fig. 1, so that the initial gap between the undeformed bodies is

$$g_0(x,y) = g_1(x,y) + g_2(x,y). \tag{9}$$

As in the Hertzian theory, we assume that the contact area is sufficiently small to permit this expression to be represented by the quadratic function

$$g_0(x,y) = \frac{x^2}{2R_I} + \frac{y^2}{2R_{II}}, \tag{10}$$

where R_I, R_{II} are the principal radii of curvature of the combined profile, as defined by Eq. (4.3) of Johnson (1985).

If the bodies are now pressed together, a contact pressure $p(x,y)$ will be developed in the contact area, which will generate elastic normal surface displacements

$$u_i(x,y,0) = \frac{1-\nu_i^2}{\pi E_i}\int\int \frac{p(\xi,\eta)d\xi d\eta}{r} \tag{11}$$

directed into the respective bodies $i = 1, 2$, where E_i is Young's modulus of the contacting body i.

The final gap between the bodies is given by

$$g(x,y) = g_0(x,y) + u_1(x,y) + u_2(x,y) + w_1(x,y) + w_2(x,y) + d, \tag{12}$$

where d is an unknown rigid body displacement. The contact problem can then be stated by noting that the gap is zero by definition in the contact area and positive outside, leading to the unilateral contact problem

$$g(x,y) = 0, \quad p(x,y) > 0, \quad (x,y) \in A, \tag{13}$$

$$p(x,y) = 0, \quad g(x,y) > 0, \quad (x,y) \notin A. \tag{14}$$

Combining Eqs. (8), (10)–(14), we then have

$$\begin{aligned}\frac{1}{\pi E^*}\int\int_A \frac{p(\xi,\eta)d\xi d\eta}{r} + \frac{(\delta_2-\delta_1)}{2\pi}\int\int_A q(\xi,\eta)\ln(r)d\xi d\eta \\ = d - g_0(x,y), \quad (x,y) \in A \\ > d - g_0(x,y), \quad (x,y) \notin A,\end{aligned} \tag{15}$$

where

$$\frac{1}{E^*} = \frac{1-\nu_1^2}{E_1} + \frac{1-\nu_2^2}{E_2}. \tag{16}$$

The corresponding total force is then given by

$$P = \int\int_A p(\xi,\eta)d\xi d\eta. \tag{17}$$

The integral equations (7) and (15) serve to determine the heat flux q and the contact pressure p, whilst Eq. (17) and the inequality in Eq. (15) determine the extent of the contact area A.

2.3. Dimensionless formulation

The number of independent parameters can be reduced by using an appropriate dimensionless representation. We first define two length scales R, a_H through the relations

$$\frac{2}{R} = \frac{1}{R_I} + \frac{1}{R_{II}}, \quad a_H = \sqrt[3]{\frac{3PR}{4E^*}} \tag{18}$$

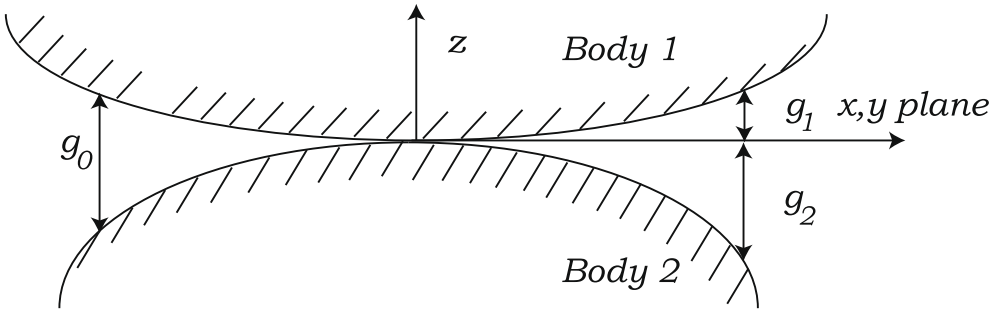

Fig. 1. Initial gap between two bodies.

and then define dimensionless coordinates $\hat{x} = x/a_H$, $\hat{y} = y/a_H$. Notice that a_H is the isothermal Hertzian contact radius for the axisymmetric case $R_I = R_{II} = R$. The governing equations can then be written as

$$\begin{aligned}\frac{1}{\pi}\int\int_{\hat{A}} \frac{\hat{p}(\hat{\xi},\hat{\eta})d\hat{\xi}\,d\hat{\eta}}{\hat{r}} + \frac{1}{2\pi}\int\int_{\hat{A}} \hat{q}(\hat{\xi},\hat{\eta})\ln(\hat{r})d\hat{\xi}\,d\hat{\eta} \\ = \hat{d} - \frac{\hat{x}^2 + R^*\hat{y}^2}{(1+R^*)}, \quad (\hat{x},\hat{y}) \in \hat{A}, \\ > \hat{d} - \frac{\hat{x}^2 + R^*\hat{y}^2}{(1+R^*)}, \quad (\hat{x},\hat{y}) \notin \hat{A},\end{aligned} \tag{19}$$

$$\frac{1}{2\pi}\int\int_{\hat{A}} \frac{\hat{q}(\hat{\xi},\hat{\eta})d\hat{\xi}\,d\hat{\eta}}{\hat{r}} = \Theta, \tag{20}$$

$$\int\int_{\hat{A}} \hat{p}(\hat{\xi},\hat{\eta})d\hat{\xi}\,d\hat{\eta} = \frac{4}{3}, \tag{21}$$

where

$$\begin{aligned}&R^* = \frac{R_I}{R_{II}}, \quad \hat{p} = \frac{pR}{E^* a_H}, \quad \hat{d} = \frac{Rd}{a_H^2}, \quad \hat{q} = (\delta_2 - \delta_1)Rq, \\ &\Theta = \frac{(\delta_2 - \delta_1)KR(T_1 - T_2)}{a_H} > 0.\end{aligned} \tag{22}$$

Notice that with this formulation, the problem is completely defined by the dimensionless parameters Θ, R^*, since $\hat{d}$ must be chosen so as to satisfy the equilibrium condition (21).

We also note that in the isothermal case $\Theta = 0$, Eq. (19) reduces to the classical Hertzian equation with solution (Johnson, 1985)

$$\hat{p}(\hat{\xi},\hat{\eta}) = \frac{2}{\pi\hat{a}\hat{b}}\sqrt{1 - \frac{\hat{x}^2}{\hat{a}^2} - \frac{\hat{y}^2}{\hat{b}^2}} \tag{23}$$

and the contact area $\hat{A}$ is an ellipse of semi-axes $\hat{a}, \hat{b}$ determined by the two simultaneous equations

$$\frac{1}{(1+R^*)} = \left(\frac{2}{\pi e^2 \hat{a}^3}\right)[K(e) - E(e)], \tag{24}$$

$$\frac{R^*}{(1+R^*)} = \left(\frac{2}{\pi e^2 \hat{a}^3}\right)\left[\frac{E(e)}{\lambda^2} - K(e)\right], \tag{25}$$

where

$$\lambda = \frac{\hat{b}}{\hat{a}}, \quad e = \sqrt{1 - \lambda^2} \tag{26}$$

and $K(e)$ and $E(e)$ are the complete elliptic integrals of the first and second kind, respectively.

3. Numerical implementation

For the numerical solution, we use a strategy based on Hartnett's solution to the isothermal contact problem (Hartnett, 1979). Suppose that a plane rectangular region, referred to as the 'blanket' region, is chosen larger than the expected contact area and this region is divided into N rectangular segments $j = 1, N$ over which the dimensionless pressure $\hat{p}_j$ and heat flux $\hat{q}_j$ are assumed to be constant. The optimal size of the blanket for a given run of the program and given computational resources is only just large enough to contain the contact area.

The contact area is defined in the numerical solution by the finite set, $\mathscr{A}$, of rectangular segments in contact. If this set were known, the corresponding heat fluxes could be found from the discrete form of Eq. (20) which can be written as

$$\frac{1}{2\pi}\sum_{j\in\mathscr{A}} C_{ij}\hat{q}_j = \Theta, \quad i \in \mathscr{A}, \tag{27}$$

where C_{ij} is a set of influence coefficients defined in Appendix A. However, the contact set $\mathscr{A}$ is determined by the *inequalities* in the discrete form of Eq. (19) which we write

$$\frac{1}{\pi}\sum_{j\in\mathscr{A}} C_{ij}\hat{p}_j + \frac{1}{2\pi}\sum_{j\in\mathscr{A}} D_{ij}\hat{q}_j = \hat{d} - \frac{\hat{x}_i^2 - R^*\hat{y}_i^2}{(1+R^*)}, \quad i \in \mathscr{A} > \hat{d} - \frac{\hat{x}_i^2 - R^*\hat{y}_i^2}{(1+R^*)}, \quad i \notin \mathscr{A}, \tag{28}$$

where D_{ij} is a set of influence coefficients appropriate to the second integral in Eq. (19) and is defined in Appendix A.

We therefore adopt an iterative solution to the problem in which Eqs. (19) and (20) are solved alternately, the contact set at the latest iteration of Eq. (19) being used in Eq. (20) and the heat fluxes q_j from the solution of Eq. (20) being taken as known in the next iteration of Eq. (19). Notice also that in the iterative solution of Eq. (19), the parameter $\hat{d}$ must be chosen to satisfy the equilibrium condition (21) which has the discrete form

$$\sum_{j\in\mathscr{A}} \hat{p}_j A_j = \frac{4}{3}, \tag{29}$$

where A_j is the area of the segment j.

3.1. Numerical validation and convergence

To validate the numerical program and also to explore the mesh refinement required to give a good description of the thermoelastic contact behaviour, we first apply the numerical method to the axisymmetric Hertzian contact problem solved analytically by Barber (1973), for which the contact area is given by Eq. (1) and the contact pressure distribution is

$$\hat{p}(\hat{r}) = \frac{2\sqrt{\hat{a}^2 - \hat{r}^2}}{\pi} + \frac{\Theta}{4}\left\{1 - \frac{8}{\pi^2}\chi_2\left(\frac{\hat{a} - \sqrt{\hat{a}^2 - \hat{r}^2}}{\hat{a} + \sqrt{\hat{a}^2 - \hat{r}^2}}\right)\right\}, \tag{30}$$

where

$$\chi_2(x) = \frac{1}{2}\int_0^x \ln\left(\frac{1+y}{1-y}\right)\frac{dy}{y} = \sum_{m=1}^{\infty}\frac{x^{2m-1}}{(2m-1)^2}. \tag{31}$$

Fig. 2 shows the percentage difference between the analytical maximum contact pressure $\hat{p}(0)$ and the numerical value as a function of the number N of elements in the contact area, for a dimensionless temperature difference $\Theta = 1$. In the same figure, we also show the percentage error in the contact radius $\hat{a}$ which is estimated in the numerical solution by equating the total contact area $\sum A_j$, $j \in \mathscr{A}$ to $\pi\hat{a}^2$. In the following numerical results, the number of elements in the contact area is above 14,000.

4. Non-axisymmetric results

Numerical results were obtained for various values of the dimensionless parameters R^*, Θ. Fig. 3 shows pressure contours and the extent of the contact area for $R^* = 5/3$ and various values of the temperature difference Θ. In the isothermal case $\Theta = 0$, the classical Hertzian analysis applies and the contact area is elliptical. As Θ is increased, the contact area gets smaller and its ellipticity is reduced. The solution can be seen as a trade-off between the elastic and thermoelastic terms in Eq. (19). The limit $\Theta \to \infty$ can be approached either by allowing the temperature difference to increase without limit or by allowing $R \to \infty$, which corresponds to the contact between two bodies with plane surfaces. In the latter case, it is clear that the ratio R^* becomes irrelevant and the contact area is circular, being given by Eq. (1) as

$$\hat{a} = \sqrt{\frac{2\pi}{3\Theta}}, \tag{32}$$

or in dimensional terms

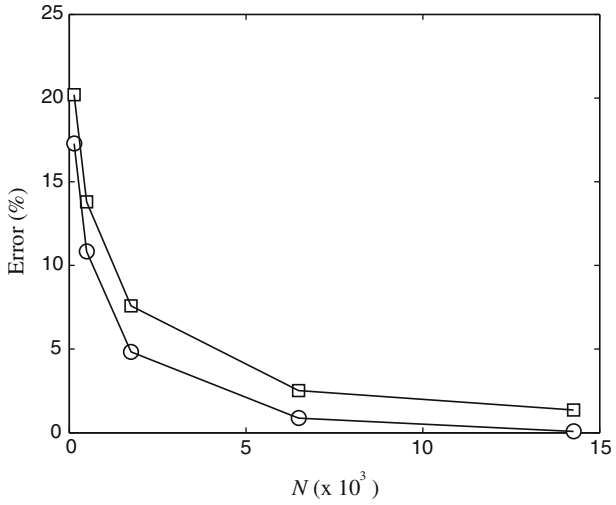

Fig. 2. Percentage difference between the analytical and numerical values of maximum contact pressure (□) and contact radius (○) as a function of the number of elements defining the contact area.

$$a = \sqrt{\frac{\pi P}{2E^*(\delta_2 - \delta_1)(T_1 - T_2)K}}. \tag{33}$$

5. Elliptical approximation to the contact area

Fig. 3 shows that the contact area remains approximately elliptical for all values of Θ and this suggests an alternative approximate analytical approach to the problem. Suppose we assume the contact area $\hat{A}$ to be an ellipse of prescribed dimensionless semi-axes $\hat{a}, \hat{b}$. Eq. (20) then defines a classical problem in potential theory with solution

$$\hat{q}(\hat{\xi}, \hat{\eta}) = \frac{\Theta}{\hat{b}K(e)\sqrt{1 - \hat{\xi}^2/\hat{a}^2 - \hat{\eta}^2/\hat{b}^2}}. \tag{34}$$

We next calculate the second integral term in Eq. (19), which we write as

$$\hat{w}(\hat{x}, \hat{y}) = \frac{\Theta}{2\pi\hat{b}K(e)} \int\int_{\hat{A}} \frac{\ln(\hat{r}) d\hat{\xi}\, d\hat{\eta}}{\sqrt{1 - \hat{\xi}^2/\hat{a}^2 - \hat{\eta}^2/\hat{b}^2}}. \tag{35}$$

This integral is evaluated in Appendix B, after which we approximate $\hat{w}(\hat{x}, \hat{y})$ by the quadratic function

$$\hat{w}^*(\hat{x}, \hat{y}) = C_0 + C_1\hat{x}^2 + C_2\hat{y}^2. \tag{36}$$

The curvatures C_1, C_2 are chosen so as to agree with the exact result at the center and at the ends of the major and minor axes of the ellipse $(\pm\hat{a}, 0), (0, \pm\hat{b})$, giving

$$C_1 = \frac{\hat{w}(\hat{a}, 0) - \hat{w}(0, 0)}{\hat{a}^2}, \quad C_2 = \frac{\hat{w}(0, \hat{b}) - \hat{w}(0, 0)}{\hat{b}^2}. \tag{37}$$

The constant C_0 can be wrapped into $\hat{d}$ in Eq. (19). This technique was used by Yevtushenko and Kulchytsky-Zhyhailo (1996) for the related problem of thermoelastic contact where heat is generated at the interface due to frictional sliding.

With this approximation, Eq. (19) once again defines a classical Hertzian contact problem for $\hat{p}$ and the semi-axes of the contact ellipse are defined by the modified equations

$$\frac{1}{(1 + R^*)} + \frac{\Theta}{\lambda\hat{a}K(e)}\Phi\left(\frac{1}{\lambda}\right) = \frac{2}{\pi e^2\hat{a}^3}[K(e) - E(e)], \tag{38}$$

$$\frac{R^*}{(1 + R^*)} + \frac{\Theta}{\lambda\hat{a}K(e)}\Phi(\lambda) = \frac{2}{\pi e^2\hat{a}^3}\left[\frac{E(e)}{\lambda^2} - K(e)\right], \tag{39}$$

where

$$\Phi(\lambda) = \frac{1}{\pi}\int_0^{\pi/2}\left[\cos\varphi \operatorname{arctanh}(\cos\varphi) + \frac{1}{2}\ln(1 - \cos^2\varphi)\right] \times \frac{d\varphi}{\left(\lambda^2\sin^2\varphi + \cos^2\varphi\right)}. \tag{40}$$

In the axisymmetric limit $R^* = 1, \lambda = 1, e = 0$ and Eqs. (38) and (39)both reduce to

$$\hat{a}^3 + \Theta\Phi(1)\hat{a}^2 = 1, \tag{41}$$

with $\Phi(1) = \pi/2(1 - \ln(2))$. Comparing with the exact expression (1), we find that the error in the multiplier on the second term is 0.94%.

6. Results

Fig. 4 shows the dimensionless major axis $\hat{a}$ as a function of Θ for various values of R^* as predicted by the numerical solution and by the approximate solution of Eqs. (38) and (39).

To compare predictions of the shape of the contact area, we present values of the ratio $\lambda = \hat{b}/\hat{a}$ as a function of Θ for various values of R^* in Fig. 5. It is clear that thermoelastic effects tend to reduce the ellipticity of the contact area. In the limit $\Theta \to \infty$, the contact area becomes circular and the solution is adequately described by the axisymmetric theory. Notice that the approximate theory consistently overestimates λ (and hence underestimates the ellipticity e) at larger values of Θ. Numerical predictions of λ in the isothermal (Hertzian) case $\Theta = 0$ are extremely good, so we conclude that this discrepancy is a real effect and not attributable to discretization.

To obtain a more robust characterization of the shape of the contact area predicted by the numerical solution, we first defined the points on the discrete boundary in the form of a piecewise continuous function $\hat{r}(\theta)$ in polar coordinates. If the contact area were a true ellipse, we would have

$$\frac{\hat{r}^2\cos\theta^2}{\hat{a}^2} + \frac{\hat{r}^2\sin\theta^2}{\lambda^2\hat{a}^2} = 1 \tag{42}$$

and hence

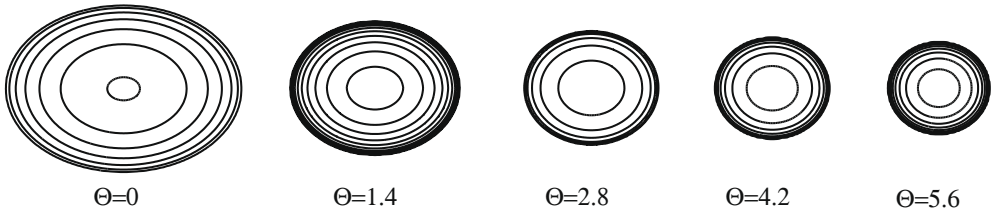

Fig. 3. Contact pressure distribution and extent of the contact area for $R^* = 5/3$ and various values of the dimensionless temperature difference Θ.

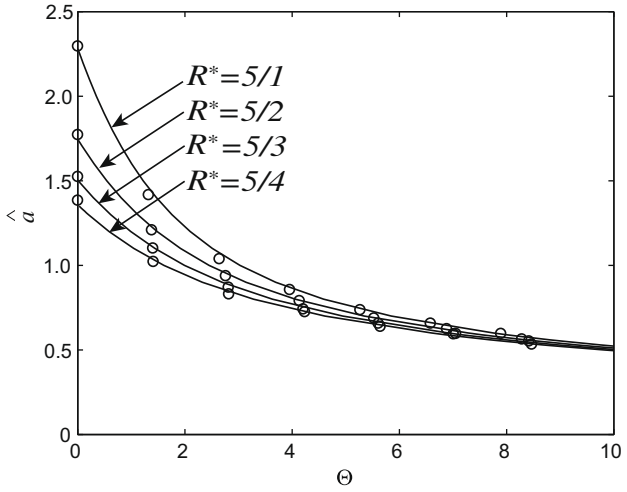

Fig. 4. Dimensionless major axis of the contact area ($\hat{a}$) as a function of dimensionless temperature difference Θ. The circles and the solid lines represent the numerical and approximate analytical solutions, respectively.

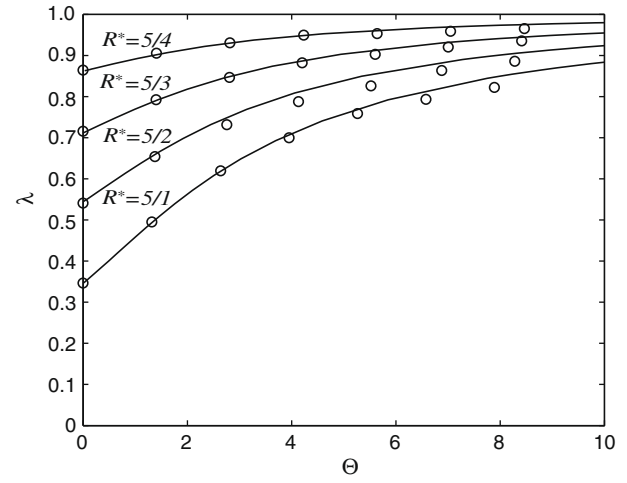

Fig. 5. The ratio of major/minor axes of the contact area ($\lambda = b/a$) as a function of dimensionless temperature difference Θ. The circles and the solid lines represent the numerical and approximate analytical solutions, respectively.

$$\hat{r}(\theta) = \sqrt{\frac{2\hat{a}^2\lambda^2}{\left[(1+\lambda^2)-(1-\lambda^2)\cos(2\theta)\right]}}. \tag{43}$$

It then follows that the Fourier series representation of the function

$$f(\theta) \equiv \frac{1}{\hat{r}^2} = \sum_{n=0}^{\infty} c_{2n}\cos(2n\theta). \tag{44}$$

would have only two non-zero coefficients, c_0, c_2.

Table 1 shows the first four coefficients of this series for $R^* = 5$ and several values of Θ. In the first two columns, we compare the numerical values of the coefficients with the exact (Hertzian) values from Eqs. (43) and (44). The magnitude of the higher coefficients $c_4, c_6, \ldots$ in the numerical solution for $\Theta = 0$ provides an indication of the error due to discretization. For $\Theta \neq 0$, the third coefficient c_4 is significantly larger than this error and hence describes a real effect. Its sign is such as to indicate an elongation of the contact area on the major and minor axes and a reduction in $\hat{r}(\theta)$ at $\theta = 45^\circ$. However, the higher coefficients are still much smaller than c_0, c_2 indicating that the contact area remains predominantly elliptical.

Table 1
Comparison of Fourier coefficients for the series (44) with the approximate analytical solution.

Θ	0		3.95	7.89
	Hertzian	Numerical		
c_0	1.42	1.41	3.39	5.56
c_2	−1.12	−1.11	−1.16	−1.08
c_4	0	0.0049	−0.016	−0.053
c_6	0	−0.0059	0.012	0.045
c_8	0	0.0074	−0.019	−0.003

7. Conclusion

We have presented a numerical solution and an approximate analytical solution to the problem of the general thermoelastic Hertzian contact problem with heat flow through the contact area driven by a temperature difference between the extremities of the two contacting bodies. The solution is characterized by only two dimensionless parameters, the ratio R^* of principal curvatures of the bodies which governs the ellipticity of the contact area in the isothermal (Hertzian) case, and a dimensionless temperature difference Θ.

The contact area remains substantially elliptical for all values of Θ, but the ellipticity decreases with increasing Θ, approaching the limiting axisymmetric solution as $\Theta \to \infty$. The analytical approximation, based on a technique due to Yevtushenko and Kulchytsky-Zhyhailo (1996), underestimates the ellipticity at intermediate values of Θ.

Appendix A. C_{ij} and D_{ij} of Eq. (28)

If x_j, y_j are the coordinates of the center of the rectangular contact element j of dimensions $2h \times 2l$, the influence coefficients C_{ij}, D_{ij} of Eqs. (27) and (28) are

$$\begin{aligned}
C_{ij} =& (\hat{x}_j-\hat{x}_i+\hat{h})\ln\left[\frac{(\hat{y}_j-\hat{y}_i+\hat{l})+\sqrt{(\hat{y}_j-\hat{y}_i+\hat{l})^2+(\hat{x}_j-\hat{x}_i+\hat{h})^2}}{(\hat{y}_j-\hat{y}_i-\hat{l})+\sqrt{(\hat{y}_j-\hat{y}_i-\hat{l})^2+(\hat{x}_j-\hat{x}_i+\hat{h})^2}}\right] \\
&+(\hat{x}_j-\hat{x}_i-\hat{h})\ln\left[\frac{(\hat{y}_j-\hat{y}_i-\hat{l})+\sqrt{(\hat{y}_j-\hat{y}_i-\hat{l})^2+(\hat{x}_j-\hat{x}_i-\hat{h})^2}}{(\hat{y}_j-\hat{y}_i+\hat{l})+\sqrt{(\hat{y}_j-\hat{y}_i+\hat{l})^2+(\hat{x}_j-\hat{x}_i-\hat{h})^2}}\right] \\
&+(\hat{y}_j-\hat{y}_i+\hat{l})\ln\left[\frac{(\hat{x}_j-\hat{x}_i+\hat{h})+\sqrt{(\hat{y}_j-\hat{y}_i+\hat{l})^2+(\hat{x}_j-\hat{x}_i+\hat{h})^2}}{(\hat{x}_j-\hat{x}_i-\hat{h})+\sqrt{(\hat{y}_j-\hat{y}_i+\hat{l})^2+(\hat{x}_j-\hat{x}_i-\hat{h})^2}}\right] \\
&+(\hat{y}_j-\hat{y}_i-\hat{l})\ln\left[\frac{(\hat{x}_j-\hat{x}_i-\hat{h})+\sqrt{(\hat{y}_j-\hat{y}_i-\hat{l})^2+(\hat{x}_j-\hat{x}_i-\hat{h})^2}}{(\hat{x}_j-\hat{x}_i+\hat{h})+\sqrt{(\hat{y}_j-\hat{y}_i-\hat{l})^2+(\hat{x}_j-\hat{x}_i+\hat{h})^2}}\right],
\end{aligned} \tag{45}$$

$$\begin{aligned}
D_{ij} =& \left(\hat{h}-(\hat{x}_j-\hat{x}_i)\right)\left(\hat{l}+(\hat{y}_j-\hat{y}_i)\right)\ln\{(\hat{h}-(\hat{x}_j-\hat{x}_i))^2+(\hat{l}+(\hat{y}_j-\hat{y}_i))^2\} \\
&+(\hat{h}+(\hat{x}_j-\hat{x}_i))(\hat{l}+(\hat{y}_j-\hat{y}_i))\ln\{(\hat{h}+(\hat{x}_j-\hat{x}_i))^2+\left(\hat{l}+(\hat{y}_j-\hat{y}_i)\right)^2\} \\
&+\left(\hat{h}+(\hat{x}_j-\hat{x}_i)\right)\left(\hat{l}-(\hat{y}_j-\hat{y}_i)\right)\ln\{(\hat{h}+(\hat{x}_j-\hat{x}_i))^2+\left(\hat{l}-(\hat{y}_j-\hat{y}_i)\right)^2\} \\
&+\left(\hat{h}-(\hat{x}_j-\hat{x}_i)\right)\left(\hat{l}-(\hat{y}_j-\hat{y}_i)\right)\ln\{(\hat{h}-(\hat{x}_j-\hat{x}_i))^2+(\hat{l}-(\hat{y}_j-\hat{y}_i))^2\} \\
&+(\hat{h}+(\hat{x}_j-\hat{x}_i))^2\left[\arctan\left(\frac{\hat{l}+(\hat{y}_j-\hat{y}_i)}{\hat{h}+(\hat{x}_j-\hat{x}_i)}\right)+\arctan\left(\frac{\hat{l}-(\hat{y}_j-\hat{y}_i)}{\hat{h}+(\hat{x}_j-\hat{x}_i)}\right)\right]
\end{aligned}$$

$$+(\hat{l}+(\hat{y}_j-\hat{y}_i))^2\left[\arctan\left(\frac{\hat{h}-(\hat{x}_j-\hat{x}_i)}{\hat{l}+(\hat{y}_j-\hat{y}_i)}\right)+\arctan\left(\frac{\hat{h}+(\hat{x}_j-\hat{x}_i)}{\hat{l}+(\hat{y}_j-\hat{y}_i)}\right)\right]$$
$$+\left(\hat{l}-(\hat{y}_j-\hat{y}_i)\right)^2\left[\arctan\left(\frac{\hat{h}-(\hat{x}_j-\hat{x}_i)}{\hat{l}-(\hat{y}_j-\hat{y}_i)}\right)+\arctan\left(\frac{\hat{h}+(\hat{x}_j-\hat{x}_i)}{\hat{l}-(\hat{y}_j-\hat{y}_i)}\right)\right]$$
$$+(\hat{h}-(\hat{x}_j-\hat{x}_i))^2\left[\arctan\left(\frac{\hat{l}+(\hat{y}_j-\hat{y}_i)}{\hat{h}-(\hat{x}_j-\hat{x}_i)}\right)+\arctan\left(\frac{\hat{l}-(\hat{y}_j-\hat{y}_i)}{\hat{h}-(\hat{x}_j-\hat{x}_i)}\right)\right]-12\hat{h}\hat{l} \tag{46}$$

Appendix B. Evaluation of Eq. (35)

Following Yevtushenko and Kulchytsky-Zhyhailo (1996), we note that

$$I_1(\hat{x},\hat{y})\equiv\int_{-\infty}^{\infty}\int_{-\infty}^{\infty}f(\hat{\xi},\hat{\eta})\ln(\hat{r})d\hat{\xi}d\hat{\eta}=\int_{-\infty}^{\infty}\int_{-\infty}^{\infty}\frac{\bar{f}(s,t)e^{\imath(\hat{x}s+\hat{y}t)}ds\,dt}{(s^2+t^2)}, \tag{47}$$

where

$$\bar{f}(s,t)=\int_{-\infty}^{\infty}\int_{-\infty}^{\infty}f(\hat{\xi},\hat{\eta})e^{-\imath(\hat{\xi}s+\hat{\eta}t)}d\hat{\xi}d\hat{\eta} \tag{48}$$

is the double Fourier transform of $f(\hat{\xi},\hat{\eta})$.

For the integral in Eq. (35), we have

$$\bar{f}(s,t)=\int\int_{\hat{A}}\frac{e^{-\imath(\hat{\xi}s+\hat{\eta}t)}d\hat{\xi}d\hat{\eta}}{\sqrt{1-\hat{\xi}^2/\hat{a}^2-\hat{\eta}^2/\hat{b}^2}}=\int\int_{\hat{A}}\frac{\cos(\hat{\xi}s+\hat{\eta}t)d\hat{\xi}d\hat{\eta}}{\sqrt{1-\hat{\xi}^2/\hat{a}^2-\hat{\eta}^2/\hat{b}^2}} \tag{49}$$

and the ellipse $\hat{A}$ can be mapped to the unit circle using the change of variable $\hat{\xi}=\hat{a}p\cos\varphi,\hat{\eta}=bp\sin\varphi$, giving

$$\bar{f}(s,t)=\hat{a}\hat{b}\int_0^1\frac{p\,dp}{\sqrt{1-p^2}}\int_0^{2\pi}\cos\left(p(\hat{a}s\cos\varphi+\hat{b}t\sin\varphi)\right)d\varphi$$
$$=\frac{\pi\sqrt{2\pi}\hat{a}\hat{b}}{\left(\hat{a}^2s^2+\hat{b}^2t^2\right)^{1/4}}J_{1/2}\left(\sqrt{\hat{a}^2s^2+\hat{b}^2t^2}\right), \tag{50}$$

using Gradshteyn and Ryzhik (1980), 3.937.2 and 6.567.1.

Using this result in Eq. (47), we obtain

$$I_1=\pi\sqrt{2\pi}\hat{a}\hat{b}\int_{-\infty}^{\infty}\int_{-\infty}^{\infty}\frac{J_{1/2}\left(\sqrt{\hat{a}^2s^2+\hat{b}^2t^2}\right)\cos(\hat{x}s+\hat{y}t)ds\,dt}{(s^2+t^2)\left(\hat{a}^2s^2+\hat{b}^2t^2\right)^{1/4}}, \tag{51}$$

but this integral is unbounded because of the behaviour of the integrand at the origin. This is to be expected, since if the net heat flow into a body is not zero, the 'rigid-body' thermoelastic displacement of the heated region is unbounded relative to the point at infinity (Barber, 1971). However, only the shape of the thermoelastically distorted surface plays a rôle in the contact problem, and the integral

$$I_2\equiv\frac{1}{\pi\sqrt{2\pi}\hat{a}\hat{b}}\frac{\partial I_1}{\partial\hat{x}}$$
$$=-\int_{-\infty}^{\infty}\int_{-\infty}^{\infty}\frac{J_{1/2}\left(\sqrt{\hat{a}^2s^2+\hat{b}^2t^2}\right)\sin(\hat{x}s+\hat{y}t)s\,ds\,dt}{(s^2+t^2)\left(\hat{a}^2s^2+\hat{b}^2t^2\right)^{1/4}} \tag{52}$$

is bounded. Using the change of variable $p\cos\varphi=\hat{a}s,p\sin\varphi=\hat{b}t$, we then obtain

$$I_2=-\hat{b}\int_0^{2\pi}\frac{\cos\varphi\,d\varphi}{\hat{a}^2\sin^2\varphi+\hat{b}^2\cos^2\varphi}\int_0^{\infty}\frac{J_{1/2}(p)\sin(p\psi)dp}{p^{1/2}}$$
$$=-\frac{\hat{b}\sqrt{2}}{\sqrt{\pi}}\int_0^{2\pi}\frac{\psi F(1,1/2,3/2,\psi^2)\cos\varphi\,d\varphi}{\hat{a}^2\sin^2\varphi+\hat{b}^2\cos^2\varphi} \tag{53}$$

from Gradshteyn and Ryzhik (1980), 6.699.1, where

$$\psi=\frac{x}{\hat{a}}\cos\varphi+\frac{y}{\hat{b}}\sin\varphi \tag{54}$$

and $F(\alpha,\beta,\gamma,x)$ is the Gauss hypergeometric function.

Using Gradshteyn and Ryzhik (1980), 9.121.1, 9.121.7, and 9.137.3 and results from Yevtushenko and Kulchytsky-Zhyhailo (1996), we obtain

$$\psi F(1,1/2,3/2,\psi^2)=\operatorname{arctanh}(\psi)=\frac{1}{2}\ln\left(\frac{1+\psi}{1-\psi}\right) \tag{55}$$

and hence we can write

$$\frac{\partial I_1}{\partial\hat{x}}=\pi\sqrt{2\pi}\hat{a}\hat{b}I_2=-2\pi\hat{a}\hat{b}^2\int_0^{2\pi}\frac{\operatorname{arctanh}(\psi)\cos\varphi\,d\varphi}{\hat{a}^2\sin^2\varphi+\hat{b}^2\cos^2\varphi}. \tag{56}$$

A similar procedure can be used to determine $\partial I_1/\partial\hat{y}$ after which we deduce that the integral I_1 has the form

$$I_1=-\pi\hat{a}^2\hat{b}^2\int_0^{2\pi}\frac{[\psi\operatorname{arctanh}(\psi)+\frac{1}{2}\ln(1-\psi^2)]d\varphi}{\hat{a}^2\sin^2\varphi+\hat{b}^2\cos^2\varphi}, \tag{57}$$

apart from an 'infinite' constant which can be wrapped into $\hat{d}$.

References

Clausing, A.M., 1966. Heat transfer at the interface between dissimilar metals – the influence of thermal strain. International Journal of Heat and Mass Transfer 9, 791–801.

Barber, J.R., 1971. The solution of heated punch problems by point source methods. International Journal Engineering Science 9, 1165–1170.

Barber, J.R., 1973. Indentation of the semi-infinite elastic solids by a hot sphere. International Journal of Mechanical Science 15, 813–819.

Barber, J.R., 1978. Contact problems involving a cooled punch. Journal of Elasticity 8, 409–423.

Kulchytsky-Zhyhailo, R.D., Olesiak, Z.S., Yevtushenko, O.O., 2001. On thermal contact of two axially symmetric elastic solids. Journal of Elasticity 63, 1–17.

Gradshteyn, I.S., Ryzhik, I.M., 1980. Tables of Integrals Series and Products. Academic Press, New York.

Hartnett, M.J., 1979. Analysis of contact stresses in rolling element bearings. Journal of Lubrication Technology – Transaction of ASME 101, 105–109.

Johnson, K.L., 1985. Contact Mechanics. Cambridge University Press, Cambridge, MA.

Yevtushenko, A.A., Kulchytsky-Zhyhailo, R.D., 1996. Approximation solution of the thermoelastic contact problem with frictional heating in the general case of the profile shape. Journal of the Mechanics and Physics of Solids 44, 243–250.